

Chronology of alluvial terrace sediment accumulation and incision in the Pativilca Valley, western Peruvian Andes

Camille Litty^{1*}, Fritz Schlunegger¹, Naki Akçar¹, Romain Delunel¹, Marcus Christl², Christof Vockenhuber²

¹ *Institute of Geological Sciences, University of Bern, Baltzerstrasse 1+3, CH- 3012 Bern.*

² *Laboratory of Ion Beam Physics, ETH Zurich, Zurich, Switzerland*

* *Current address: Univ. Grenoble Alpes, IUGA, ISTerre, 38000 Grenoble, France*

ABSTRACT

The incision and aggradation of the Pativilca alluvial fan delta system in the western Peruvian Andes through Quaternary time can be traced in detail using well-exposed fill terraces studied by a combination of cosmogenic nuclide dating, terrace mapping and paleo-erosion rate calculations. Two alluvial terraces have been dated through depth-profile exposure dating using in-situ ¹⁰Be. The dating results return an age for the abandonment of the terrace at 200 ± 90 ka in Pativilca and $1.2 \text{ Ma} \pm 0.3 \text{ Ma}$ in Barranca. These new ages complete the database of previously dated terrace fills in the valley. Together with the results of the terrace mapping and the absolute ages of the terraces, we show that the valley fills are made up of at least four terraces; two terraces near the city of Pativilca and two terraces in the city of Barranca. While previous studies have shown two periods of sediment aggradation, one period around 100 ka (Barranca) and another period around 30 ka (Pativilca), our new results show two additional periods of sediment aggradation and subsequent incision that have not been reported before. Finally, paleo-erosion rates at the time of the deposition of the terrace material were calculated and compared to the available modern estimates. The paleo-erosion rates vary from 140 ± 12 m/Ma to 390 ± 40 m/Ma. The period of sediment accumulation prior to the abandonment of the terrace at 200 ka corresponds to a wet phase and a pulse of erosion. In contrast, the period of sediment accumulation prior to the abandonment of the terrace at 1.2 Ma does not

correspond to a pulse of erosion and could rather correspond to a change of the base level possibly induced by a sea-level rise.

Keywords: ^{10}Be depth-profile dating; alluvial terraces; Pativilca Valley; Western Peruvian Andes

1. Introduction

Fluvial sediments originating from mountain belts like the Andes yield important archives of past environmental or tectonic changes. The sediments can record changes in precipitation rates and climate (Litty et al., 2016; d'Arcy et al., 2017). They can also record the response to earthquake-induced landslides (McPhillips et al., 2014). The reconstruction of the timing of alluvial sediment deposition thus bears important information when the scope lies in the detection of specific climate or tectonic events as driving forces of landscape evolution. In this context, depth-profile dating based on in-situ produced ^{10}Be measured in quartz has been proven a reliable method to establish a chronology of sediment deposition (e.g., Bookhagen et al., 2006; Hidy et al., 2010). In particular, this methodology yields an age when sediment aggradation stopped and when a period of sediment accumulation was superseded by a phase of erosion and incision into the previously deposited material. ^{10}Be is the most commonly measured in situ-produced cosmogenic nuclide (Granger et al., 2013). Its dominance in geological applications stems from several factors, including the abundance of the target mineral, quartz, a standardized chemistry procedure (Kohl and Nishiizumi, 1992), a relatively simple production depth profile, and routinely good precision by accelerator mass spectrometry (AMS) (Granger, 2006). Additionally, isochron burial dating using ^{10}Be and ^{26}Al is becoming increasingly important in studies related to river terraces (e.g., Darling et al., 2012; Erlanger et al., 2012; Akçar et al., 2017). Isochron-burial dating yields in an age when the investigated material accumulated. It is thus a variation of traditional burial dating methods. Ages, or alternatively the burial times of sediment, are determined using the difference between the cosmogenic $^{26}\text{Al}/^{10}\text{Be}$ surface production ratio at the time of burial and the $^{26}\text{Al}/^{10}\text{Be}$ ratio measured in buried sediments (Granger, 2006). Sediments of alluvial terrace deposits with flat tops are ideal for surface exposure dating and isochron burial dating: they are persistent, easily identifiable as surfaces that were formed at a specific time and that have been isolated from the fluvial system since deposition. Because they

are typically coarse-grained, well drained, and nearly flat, they can be remarkably well preserved and unaffected by erosion, especially in arid environments like in the western side of the Peruvian Andes (Litty et al., 2017a; Reber et al., 2017).

Alluvial terrace sequences are common features along the coastal margin between Peru and northern Chile. They are located particularly in lower valley reaches near to the Pacific coast (Steffen et al., 2009, 2010; Trauerstein et al., 2014; Litty et al., 2017a). Climate change has been considered to have controlled pulses of erosion on the western Andean margin through the increase in mean surface runoff resulting either in sediment accumulation along stream segments close to the Pacific coast (Bekaddour et al., 2014; Norton et al., 2016), or in surface erosion in upstream segments of major rivers (Veit et al., 2016). These climate-driven changes have been interpreted as being the main driving force controlling the sediment accumulation and the formation of cut-and-fill terraces on the western Andean margin (Norton et al., 2016). In the Pativilca Valley, situated on the western margin of the Peruvian Andes at about 10°S (Fig. 1A), a terrace sequence has been previously dated through infrared stimulated luminescence (IRSL) techniques (Trauerstein et al., 2014). The results have disclosed the occurrence of at least two periods of sediment aggradation, one period spanning from 10 ka to 90 ka with an age of the samples cluster around 30 ka and another period spanning the time interval between 80 ka and 130 ka with an age estimate of the samples cluster around 110 ka (Trauerstein et al., 2014). While generally wetter climate results in fluvial incision, the results from Trauerstein et al. (2014) suggested that here wetter climate conditions do correlate with periods of fluvial aggradation.

The aim of this study is to date additional terrace deposits using in-situ terrestrial cosmogenic nuclides to complete the chronological framework and to infer the history of sediment aggradation and incision in this alluvial fan delta system. In addition concentrations of in-situ ¹⁰Be recorded by detrital quartz minerals in the terrace deposits will be used to infer the paleo-erosion rates recorded at the time when sediment accumulation occurred. These rates will be compared to the modern ones (Reber et al., 2017) to quantify the erosion in the upstream drainage basin during the phases of aggradation within the downstream valley. The final aim is to understand the factors controlling fluvial aggradation and incision in fan delta environments in the western Andes.

81

82 **2. Regional settings**

83 The Pativilca Valley is located in central Peru, about 200 km to the northwest of Lima. The
84 Rio Pativilca, which is trunk stream of the region, debouches into the Pacific at 10.7°S and 77.8°W
85 (Fig. 1A). The drainage basin has an area of about 4400 km², and the longest flow path measures
86 approximately 200 km. The upper section of the stream is characterized by a bedrock channel with a
87 steep gradient (knickzone), whereas in the lower segment the narrow valley floor is covered by
88 alluvial deposits that are thickening and widening towards the coast, giving way to an alluvial fan
89 delta. The sedimentological architecture of the deposits is characterized by amalgamated stacks of 20
90 to 50 m-thick units of poorly sorted, clast-supported conglomerates with a coarse-grained sandy
91 matrix (Fig. 1B). The clasts are subrounded and sometimes imbricated, but the sedimentary fabrics are
92 predominantly massive (Fig. 1B). The alluvial conglomerates are part of an alluvial fan delta system
93 characterized by a suite of individual fill terraces with different altitudes of the tread (Fig. 1B).

94 The precipitation pattern of South America is strongly influenced by the low level Andean jet
95 and the position of the Inter Tropical Convergence Zone (ITCZ), which experiences seasonal shifts in
96 response to insolation differences between austral summer and winter. The Andean jet transfers
97 humidity from the Pacific Ocean and the Amazon basin to the eastern margin of the Andes, and also
98 to the Altiplano and the western Andean margin (Garreaud, 2009). The Andean mountain range thus
99 acts as a major topographic barrier to the atmospheric circulation. As a result of this circulation
100 pattern, the Peruvian western margin shows an E-W contrasting precipitation pattern with high annual
101 precipitation rates up to 800 mm on the Altiplano and ~0 mm along the coast. From north to south, the
102 annual rainfall rates on the Altiplano decrease from 1000 mm near the Equator to <200 mm in
103 northern Chile. Every 2-10 yr, near the Equator, the Pacific coast is subjected to stronger precipitation
104 than the mean precipitation rates, resulting in high flood magnitude variability related to the El Nino
105 Southern Oscillation (ENSO) weather phenomenon (DeVries, 1987). Today, this phenomenon is
106 limited to the coastal area of northern Peru, but during the past, southern Peru might also have been
107 affected by such events (Lagos et al., 2008).

On orbital time scales, the position of the ITCZ has shifted in response to larger insolation and heat contrasts between the Northern and Southern Hemispheres, which has been related to the effects of shifts in the Earth's precession (Strecker et al., 2007). The results are stronger upper air easterlies and more precipitation on the Altiplano (Garreaud et al., 2003). Variations in precipitation rates and patterns led to remarkable lake level variations on the Altiplano as recorded by lake level highstands on the plateau (Ouki, Minchin and Tauca pluvial periods, e.g., Fritz et al., 2004). These climate changes have also controlled pulses of erosion and deposition on the western Andean margin (Bekaddour et al., 2014; Veit et al., 2016). Related variations in erosional fluxes have been interpreted as being the main factor controlling the formation of cut-and-fill terrace systems along the western margin of the Peruvian Andes (Norton et al., 2016).

3. Methods

3.1. Cosmogenic nuclides

Over the past 25 yr, cosmogenic nuclides have become an essential tool in Quaternary geochronology (e.g., Gosse and Phillips, 2001; Granger, 2006). Cosmogenic nuclides are produced through spallation reactions and muon capture in minerals of rocks and sediment at or near the Earth's surface (Gosse and Philips, 2001). Cosmogenic ^{10}Be and ^{26}Al can be applied to determine a post-depositional age of a geological layer using their accumulation (depth-profile dating). Alternatively, they can also be used to determine the timing of sediment accumulation through their radioactive decay (burial dating) history (e.g., Anderson et al., 1996; Repka et al., 1997; Granger and Smith, 2000; Granger and Muzikar, 2001; Wolkowinsky and Granger, 2004; Balco and Rovey, 2008; Akçar et al., 2017).

Depth-profile dating is based on the exponential decrease of cosmogenic nuclides with depth (Gosse and Philips, 2001). On the other hand, the burial dating technique uses the difference in half-lives of ^{10}Be (1.387 Ma; Korschinek et al., 2010; Chmeleff et al., 2010) and ^{26}Al (0.705 Ma; Norris et al., 1983) and thus the ^{26}Al versus ^{10}Be ratio to determine the burial time, when the pre-burial and post-burial concentrations are known or estimated (e.g., Granger and Muzikar, 2001; Akçar et al.,

2017). We followed the Erlanger et al. (2012) isochron approach where one of the advantages is the assumption that post-burial production is identical across a single stratigraphic horizon.

The collected samples (see section 3.3 for description of sample sites and sampling strategy) were processed in the Surface Exposure Laboratory of the Institute of Geological Sciences at the University of Bern following the lab protocol described in Akçar et al. (2012). The $^{10}\text{Be}/^9\text{Be}$ and $^{26}\text{Al}/^{27}\text{Al}$ AMS measurements were then performed at the Swiss Federal Institute of Technology tandem facility in Zurich (Christl et al., 2013). The long-term weighted average $^{10}\text{Be}/^9\text{Be}$ ratio of $(2.41 \pm 0.53) \times 10^{-15}$ was used for full process blank correction. Table 1 presents the samples information and cosmogenic nuclide results.

Depth-profile ages were modelled with MATLAB® using Monte Carlo simulations developed by Hidy et al. (2010). Depth-profile patterns were simulated based on exposure age, erosion rate and inheritance. Table 2 shows the input parameters for the Barranca and Pativilca depth-profile simulations. We applied no correction factor for topographic shielding. We justify this approach because there is no significant topography around the sampling sites that could block a portion of incoming cosmic radiations (Dunne et al., 1999; Gosse and Phillips, 2001), as the sampling sites are located on the widest and flattest part of the valley close to the coast. We did not consider snow cover to have a major impact on the results as the mean basin elevation of the sampled catchment is largely situated below the snow line. The ^{10}Be half-life with a value of 1.387 ± 0.012 Ma was utilized (Chmeleff et al., 2010; Korschinek et al., 2010). The local production rate was scaled to the Lal (1991) and Stone (2000) scheme using a production rate caused by spallation (SLHL: at sea-level, high latitude) of 4.01 ± 0.12 atoms $\text{g}_{\text{SiO}_2}^{-1}$ (CRONUS calculator update from v. 2.2 to v. 2.3 published by Balco in August 2016 after Balco et al., 2008; Borchers et al., 2016). Thus a site-specific spallogenic production rate of 2.5 ± 0.5 atoms $\text{g}^{-1} \text{a}^{-1}$ was obtained for Barranca and for Pativilca. We applied a bulk density ranging between 1.6 and 2.1 g cm^{-3} for the sediment samples in Barranca and Pativilca. Finally, to model a depth-profile age we simulated 100,000 profiles and used a χ^2 cut-off value of ≤ 20 for Barranca and ≤ 3 for Pativilca (Table 2).

3.2. *Paleo erosion rates*

Paleo basin-averaged erosion rates can be calculated using the cosmogenic nuclide concentrations of past sediment samples following Granger et al. (1996) and von Blanckenburg (2005). To calculate the basin averaged paleo-erosion rate, we used the ^{10}Be cosmogenic nuclide concentrations of the sand embedded in the terrace deposits after corrections have been made for shielding, post-depositional nuclide production at sample depth z , and atom loss due to radioactive decay during time t (both considered in Eq. (1); Balco et al., 2008). These equations can be used assuming: (i) The material was well mixed in the upstream basin and finally embedded in the terrace fill. This appears to be the case in the western Peruvian valleys where the fluvial processes have dominated the transport of sediment (Litty et al., 2017b), thus providing well-mixed material. (ii) The paleo-erosion is representative for the entire catchment. Indeed, the sediments of the Pleistocene terrace fills in western Peru record an origin from both the upper flat part of the catchments and the lower steep reaches (Litty et al., 2017a). (iii) The residence of the material on the hillslopes and the channels is much shorter than the erosional timescale. This is the case in the western Peruvian valleys where regolith was considered to have been rapidly stripped from hillslopes, which most likely resulted in the supply of large volumes of sediment to the trunk streams during the periods of sediment aggradation (Norton et al., 2016). (iv) The individual terraces have not experienced multiple phases of erosion and re-deposition, so that major internal unconformities are not present (von Blanckenburg, 2005). This appears to be the case in the Pativilca Valley as no unconformities in the individual terrace fills have been observed in the field.

3.3. Sampling sites

Two previously undated alluvial terrace fills were sampled for depth-profile exposure dating. These terraces are located along the lowermost reach of the Pativilca River and in the city of Barranca (Fig. 1; Table 1). At each sampling site, six samples were collected along a vertical profile from 0.9 to 4.7 m beneath the tread of the terrace in Pativilca, and from 0.4 to 3.2 m beneath the tread of the terrace in Barranca (Fig. 1A). Two to three kilograms of medium grained sand embedded between the pebbles were taken for each sample. Additionally, the lowermost samples of the two depth profiles (PAT-DP6 and BAR-DP6) were used to infer a paleo-erosion rate at the time when the sediments of

the two newly dated terraces were deposited. Two other samples (PAT-PE and BAR-PE2) were collected in two other terrace fills previously dated (Trauerstein et al., 2014) for the calculation of paleo-erosion rates (one in Pativilca and one in Barranca; Table 4). Additionally, quartz bearing clasts were sampled for isochron burial dating (Fig. 1B; Table 1). For each isochron burial site, the samples were collected from the same sedimentologic unit and from a single stratigraphic horizon following Erlanger et al. (2012). Three horizons were sampled in Barranca and two horizons have been sampled in Pativilca (Fig. 1B; Table 1). Depth-profile dating and isochron burial dating techniques have been chosen as sand lenses that are required for IRSL sampling are not present in every terrace fill.

4. Results

4.1. Cosmogenic nuclides: isochron burial dating

The measured ^{26}Al concentrations are plotted versus ^{10}Be concentrations including 2σ uncertainties (Fig. 2). The cosmogenic nuclide results are shown in Table 1. As the Al/Be ratios are higher than the surface ratio, it is not possible to calculate an isochron burial age from these samples (for details, see Erlanger et al., 2012). The surface ratio of $^{26}\text{Al}/^{10}\text{Be}$ is not constant since it depends on the time of exposure and erosion. On a banana-plot, the ratios decrease from 8.4 to ~ 3 , and a regression through these yields a surface ratio around 6.8. Therefore, in most of the isochron burial applications this ratio has been used as the surface ratio. Recently, Akçar et al. (2017) showed that this ratio varied between 7 and 12 in deeply eroding landscapes, particularly in glacial environments. However, these mechanisms fail to explain the $^{26}\text{Al}/^{10}\text{Be}$ ratios > 12 obtained in this study as glacial processes were most likely not the most important erosional mechanisms. Therefore, we tentatively attribute these ratios to the analytical problems related to the measurements of the total Al or to the quartz purification process. Given that no age can be determined from these samples; isochron burial dating is therefore not further discussed in this paper.

4.2. Cosmogenic nuclides: depth-profile dating

4.2.1. Barranca

AMS-measured $^{10}\text{Be}/^9\text{Be}$ (with uncertainties) as well as calculated ^{10}Be concentrations for each sample are shown in Table 1. The concentrations of the six sediment samples vary from $\sim 12 \times 10^5$ atoms g^{-1} for the uppermost sample to $\sim 1 \times 10^5$ atoms g^{-1} for the lowermost sample (Table 1). In Fig. 3, the ^{10}Be concentrations together with 1σ uncertainties are plotted against depth. They display an exponential decrease with depth. The simulated best fit curve through the six data points is illustrated in Fig. 4, whereas the possible solution space with a χ^2 cut-off value of ≤ 20 is shown in Fig. 5.

The simulation yields a best-fit solution to the measured nuclide concentrations for a modal depth-profile age of 1.2 ± 0.3 Ma, and a modal top erosion rate of 0.07 ± 0.02 cm ka^{-1} (Table 3A). The modal values of the age and erosion rate are similar to the mean and median values of the simulation, thus the errors of the modal values are based on the minimum and maximum values generated by the simulation. Note that the Monte Carlo simulation code requires a constraint on the net erosion on the top of the section as a modal input parameter to calculate an age (Hidy et al., 2010). This parameter is iteratively adjusted within a range of values.

4.2.2. Pativilca

The concentrations of the six sediment samples vary from $\sim 86 \times 10^4$ atoms g^{-1} for the uppermost sample to $\sim 44 \times 10^4$ atoms g^{-1} for the lowermost sample (Table 1). In Fig. 6, the ^{10}Be concentrations together with 1σ uncertainties are plotted against depth. The best fit through the six data points is illustrated in Fig. 7, whereas the possible solution space with a χ^2 cut-off value of ≤ 3 is shown in Fig. 8.

The simulation yields a best-fit solution to the measured nuclide concentrations for a modal depth-profile age of 200 ± 90 ka, a modal top erosion of $0.48+0.41-0.13$ cm ka^{-1} and an inheritance of $35,100+8700-8000$ atoms g^{-1} (Table 3B). The modal values are similar to the mean and median values of the simulation, thus the errors of the modal values are based on the minimum and maximum values generated by the simulation.

The results of the depth-profile dating return a surface exposure age of ~1.2 Ma in Barranca and of ~200 ka in Pativilca. These results show minimum ages when the accumulation of material has terminated and when dissection of the previously deposited material started, yielding in the formation of a terrace level. These two periods when sediment aggradation was superseded by dissection, have not been dated before. These new results together with the ones from Traustein et al. (2014) suggest the occurrence of at least four terraces referred to as T1 to T4 from older to younger (Figs. 9 and 10A), corresponding to at least four different periods of sediment accumulation. Terrace deposits were correlated on the basis of landscape position, tread altitude and absolute dating (Figs. 9 and 10A).

4.3. *Paleo-erosion rates*

The in-situ ^{10}Be analytical data together with the inferred paleo-erosion rates recorded by the alluvial terrace sediments are presented in Table 4. The paleo-erosion rate values are $143 \pm 12 \text{ m Ma}^{-1}$ at the time of the accumulation of the terrace deposits T1 (~1.2 Ma ago), $302 \pm 28 \text{ m Ma}^{-1}$ at the time when terrace material T2 was deposited, $392 \pm 40 \text{ m Ma}^{-1}$ at the time of the deposition of the terrace sediments T3, and finally $297 \pm 29 \text{ m Ma}^{-1}$ at the time terrace T4 was constructed (Fig. 10B). In addition, Reber et al. (2017) reported a modern catchment-averaged denudation rate of $260 \pm 23 \text{ m Ma}^{-1}$.

5. Discussion

5.1. *Chronology of sediment accumulation and incision*

The fluvial aggradation and subsequent incision in the Pativilca Valley has occurred in multiple episodes through the Quaternary (Figs. 9 and 10). Figure 11 shows the position of the active river and the position of the sediment accumulation during the periods of aggradation. Our dating results imply that the sediments of terrace T1 in Barranca have been deposited prior to 1.2 Ma. The aggradation then ceased and the tread formation began ~1.2 Ma ago (terrace T1; Fig. 11A). During the period of the terrace fill, the erosion rate was two times lower than the modern rate (Fig. 12). Following this, for approximately 1 Ma, either a period of no sedimentation occurred in the valley or no sediments have been preserved. The river then moved its course towards Pativilca. The sediments

of terrace T2 in Pativilca have been deposited prior to 200 ka. The accumulation of sediment then stopped and exposed the terrace tread at around 200 ka (terrace T2; Fig. 11B). During the period of sediment accumulation, the erosion rate was up to $\sim 300 \text{ m.Ma}^{-1}$ (Fig. 12). The river bed again changed its course towards Barranca, and a phase of accumulation occurred around 100 ka (deposition of the sediment of T3; Fig. 11C; Trauerstein et al., 2014). In this period, the erosion rate was at its highest ($\sim 400 \text{ m Ma}^{-1}$; Fig. 12). Finally, the lobe of the Pativilca fan delta moved back towards the city of Pativilca close to its current course, and a phase of aggradation occurred from 10 to 45 ka ago (deposition of the sediment of T4; Fig. 11D; Trauerstein et al., 2014). During this period, the catchment-wide denudation rate dropped back to $\sim 300 \text{ m Ma}^{-1}$ (Fig. 12). This phase was followed by a period of incision exposing the tread and riser of terrace level T4. Today the erosion rate is slightly lower than during the past at $\sim 200 \text{ ka}$ (Fig. 12) and the river appears to be incising.

5.2. *Implications for climate variability as controls on cyclic deposition and erosion*

A stratigraphic record of river terrace sediments is formed and preserved as a stream changes its activity between incision, lateral planation, and aggradation (Pederson et al., 2006). These fill terraces in the Pativilca Valley represent a relatively complete archive of both incision and deposition. They can be used to understand the response to climate or to other driving forces that have an impact on the balance between sediment transport and deposition (Pederson et al., 2006). These terrace fills have been formed in the alluvial fan delta of the Pativilca River and they might also record the change in the position of the different lobes of the delta through shifts in transport and sediment capacity. Alternatively, a phase of accumulation requires the availability of sediments on the hillslopes to be eroded, transported and deposited (Hancock and Anderson, 2002). This implies that the river experiences an increase in the ratio between sediment supply and the stream's capacity to control the deposition the supplied material (Tucker and Slingerland, 1997). The youngest period of sediment accumulation ranging from 10 to 45 ka (terrace T4) could correspond to the wet intervals recorded by the Minchin (47.8–36 ka ago) and Tauca (26–14.9 ka ago) paleolakes (Fritz et al., 2004). The period of sediment accumulation ranging from 80 to 130 ka (terrace T3) could correspond to the wet period characterized by the Ouki paleolakes (120–98 ka ago; Fritz et al., 2004). These two periods of

299 sediment accumulation previously dated by Trauerstein et al. (2014) are thus correlated with phases of
300 enhanced precipitation with higher water discharge in the river. These wet conditions could have been
301 induced by summer insolation forcing of the South American summer monsoon at precessional time-
302 scales (Baker et al., 2001a,b). Indeed, the precession together with the obliquity has been considered
303 to control the seasonal cycles of insolation (Milankovitch, 1941). The wettest phases, and hence the
304 highest lake levels (Bills et al., 1994; Sylvestre et al., 1999; Placzek et al., 2006), were additionally
305 forced by warm North Atlantic sea surface temperatures (Baker et al., 2001a). These climate changes
306 were also used to explain the pulses of upland erosion and deposition in the stream valleys on the
307 western Andean margin (Bekaddour et al., 2014), which agree with our data of relative fast paleo-
308 erosion rates recorded by these two terraces. Indeed, the 10-45 ka denudation rate was >10% higher
309 than the modern one and the 80-130 ka denudation rate was even >30% higher than the modern rates
310 (Fig. 12). Fluvial aggradation is here correlated with wetter climates and an increased sediment supply
311 from the uplands. However, we also note that wetter climates can result in fluvial incision and terrace
312 formation because of greater stream discharge (Veit et al., 2016), provided that the hillslopes have
313 been depleted of material (Norton et al., 2016). In our case, the start of the incision phases could then
314 correspond to the end of the pluvial period and the time of decrease of the supply of sediment to the
315 river. Alternatively, it is also possible that erosional recycling of the terrace material started within the
316 pluvial periods, when the preceding phase of rapid hillslope erosion resulted in the depletion of the
317 sediment reservoirs, yielding high ratios between water and sediment fluxes in the trunk stream. The
318 Altiplano lake sediment cores do not record climatic variations older than 130 ka (Placzek et al.,
319 2006). In this context, we cannot correlate the two older periods of sediment accumulation (prior to
320 ~200 ka and prior to ~1.2 Ma) to any lake level variations. However, the high paleo-erosion rate
321 calculated for the newly dated fills of the terrace T2 (~15% higher than the modern one) appears also
322 to correspond to a pulse of upland erosion, which could point towards a period of wet conditions.
323 Support for this interpretation is provided by the periodicity of about 100 ka for this orbital-induced
324 summer insolation forcing (Milankovitch, 1941; Lisiecki, 2010; Abe-Ouchi et al., 2013). If this
325 interpretation is valid, then the ages of 100 ka (T3) and 200 ka (T2) would then correspond to this 100
326 ka periodicity, suggesting that the period prior to ~200 ka might also have corresponded to a wet

phase on the Altiplano. The oldest dated period of sediment accumulation (terrace T1) does not record a distinct pulse of erosion as the calculated paleo erosion rate was twice as low as the modern one. The production of sediments on the hillslopes through weathering and erosion can occur through an increase in precipitation rates (e.g., Bookhagen et al., 2005; Norton et al., 2016), for which there is no evidence from the records reported here indicating that sediment accumulation of the terrace T1 has not been induced by a phase of enhanced precipitation. Alternatively, this T1 phase of accumulation could have occurred in response to a rise in sea level. Indeed, a rise in sea level would cause a back filling and a super-elevation of the channel, which then would cause the delta lobe to switch positions. Supporting evidence for this interpretation has been provided by Pillans et al. (1998), who proposed that the ~1.2 Ma-old period was relatively warm and corresponded to a rising sea level. Nevertheless, we note that further research in the region is required to sustain this interpretation.

6. Conclusions

The results of the depth-profile dating together with the previously published IRSL ages (Trauerstein et al., 2014) disclose at least four terraces located in the fan delta of the Pativilca River. The sediments of terrace T1 accumulated until ~1.2 Ma ago and terraces T2, T3 and T4 were deposited prior to ~200 ka, ~100 ka ago and ~30 ka ago respectively. Additionally, paleo-erosion rates at the time of the deposition of the terrace fills were calculated and compared to the modern rates. The modern erosion rate is ~260 mm/ka, while the paleo-erosion rates vary from ~143 mm/ka to ~391 m Ma⁻¹.

The oldest period of accumulation does not correspond to a distinct pulse of erosion and could rather correspond to a period when the sea level was rising. The three younger phases of sediment accumulation most likely correspond to wet phases and pulses of erosion in the uplands. These wet conditions were likely to have been induced by summer insolation forcing of the South American summer monsoon at precessional time scales (Baker et al., 2001a, 2001b). Generally, wetter climate results in fluvial incision caused by greater stream discharge. However, wetter climate is here correlated with fluvial aggradation due to the inferred increased sediment supply from the uplands. The abandonment of the terrace treads would then correspond to the end of the pluvial period and thus

a decrease of the sediment supplied to the river. Additionally, this long period of preservation of the alluvial sediments on a coastal area implies a constant base level after the deposition of the terrace T1 despite the occurrence of an active subduction zone.

Acknowledgements

Support in the laboratory by Julia Krbanjevic is greatly appreciated. The support by Prof. Silvia Rosas and her team (PUCP, Lima) to solve logistic problems at the customs are greatly acknowledged. This research has been supported by funds of the Swiss National Science Foundation awarded to Schlunegger (project number 155892).

References

- Abe-Ouchi, A., Saito, F., Kawamura, K., Raymo, M. E., Okuno, J. I., Takahashi, K., Blatter, H., 2013. Insolation-driven 100,000-year glacial cycles and hysteresis of ice-sheet volume. *Nature* 500(7461), 190-193.
- Akçar, N., Deline, P., Ivy-Ochs, S., Alfimov, V., Hajdas, I., Kubik, P.W., et al., 2012. The 1717 AD rock avalanche deposits in the upper Ferret Valley (Italy): a dating approach with cosmogenic ^{10}Be . *Journal of Quaternary Science* 27(4), 337–440.
- Akçar, N., Ivy-Ochs, S., Alfimov, V., Schlunegger, F., Claude, A., Reber, R., Christl, M., Vockenhuber, C., Dehnert, A., Rahn M., Schlüchter, C. 2017. Isochron-burial dating of glaciofluvial deposits: First results from the Swiss Alps. *Earth Surface Processes Landforms*. In Press.
- Anderson, R.S., Repka, J.L., Dick, G.S., 1996. Explicit treatment of inheritance in dating depositional surfaces using in situ ^{10}Be and ^{26}Al . *Geology* 24(1), 47-51.
- Baker P.A., Seltzer G.O., Fritz, S.C., Dunbar, R.B., Grove, M.J., Tapia, P.M., Cross, S.L., Rowe, H.D., Broda, J.P. 2001a. The history of South American tropical precipitation for the past 25,000 years. *Science* 291,640–643.
- Baker, P.A., Rigsby, C.A., Seltzer, G.O., Fritz, S.C., Lowenstein, T., Bacher, N., Veliz, C. 2001b. Tropical climate changes at millennial and orbital timescales on the Bolivian Altiplano. *Nature* 409, 698–701.
- Balco, G., Rovey, C.W., 2008. An isochron method for cosmogenicnuclide dating of buried soils and sediments. *American Journal of Sciences* 308, 1083–1114.
- Balco, G., Stone, J.O., Lifton, N.A., Dunai, T.J., 2008. A complete and easily accessible means of calculating surface exposure ages or erosion rates from Be-10 and Al-26 measurements. *Quaternary Geochronology* 3, 174–195.
- Bekaddour, T., Schlunegger, F., Vogel, H., Delunel, R., Norton, K. P., Akçar, N., Kubik, P., 2014. Paleo erosion rates and climate shifts recorded by Quaternary cut-and-fill sequences in the Pisco Valley, central Peru. *Earth and planetary science letters* 390, 103-115.

Bills, B.G., De Silva, S.L., Currey, D.R., Emenger, R.S., Lillquist, K.D., Donnellan, A., Worden, B., 1994. Hydro-isostatic deflection and tectonic tilting in the central Andes: Initial results of a GPS survey of Lake Minchin shorelines. *Geophysical Research Letters* 21(4), 293-296.

Bookhagen, B., Thiede, R. C., Strecker, M. R., 2005. Abnormal monsoon years and their control on erosion and sediment flux in the high, arid northwest Himalaya. *Earth and Planetary Science Letters*, 231(1), 131-146.

Bookhagen, B., Fleitmann, D., Nishiizumi, K., Strecker, M. R., Thiede, R. C., 2006. Holocene monsoonal dynamics and fluvial terrace formation in the northwest Himalaya, India. *Geology* 34(7), 601-604.

Borchers, B., Marrero, S., Balco, G., Caffee, M., Goehring, B., Lifton, N., Nishiizumi, K., Phillips, F., Schaefer, J., Stone, J., 2016. Geological calibration of spallation production rates in the CRONUS-Earth project. *Quaternary Geochronology* 31, 188–198.

Braucher, R., Merchel, S., Borgomano, J., Bourles, D.L., 2011. Production of cosmogenic radionuclides at great depth: A multi element approach. *Earth and Planetary Science Letters* 309(1), 1–9.

Chmeleff, J., von Blanckenburg, F., Kossert, K., Jakob, D., 2010. Determination of the Be-10 half-life by multicollector ICP-MS and liquid scintillation counting. *Nuclear Instruments and Methods in Physics, Research Section B: Beam Interactions with Materials and Atoms* 268.

Christl, M., Vockenhuber, C., Kubik, P.W., Wacker, L., Lachner, J., Alfimov, V., Synal, H.A., 2013. The ETH Zurich AMS facilities: Performance parameters and reference materials. *Nuclear Instruments and Methods in Physics Research Section B: Beam Interactions with Materials and Atoms* 294, 29-38.

D'arcy, M., Whittaker, A.C., Roda-Boluda, D.C., 2017. Measuring alluvial fan sensitivity to past climate changes using a self-similarity approach to grain-size fining, Death Valley, California. *Sedimentology* 64(2), 388-424.

Darling, A.L., Karlstrom, K.E., Granger, D.E., Aslan, A., Kirby, E., Ouimet, W. B., Cole, R. D., 2012. New incision rates along the Colorado River system based on cosmogenic burial dating of terraces: Implications for regional controls on Quaternary incision. *Geosphere* 8(5), 1020-1041.

DeVries, T.J., 1987, A review of geological evidence for ancient El Nino activity in Peru. *J. Geophys. Res* 92(14), 471–14

Dunne, J., Elmore, D., Muzikar, P., 1999. Scaling factors for the rates of production of cosmogenic nuclides for geometric shielding and attenuation at depth on sloped surfaces. *Geomorphology* 27, 3–11.

Erlanger, E.D., Granger, D.E., Gibbon, R. J., 2012. Rock uplift rates in South Africa from isochron burial dating of fluvial and marine terraces. *Geology* 40(11), 1019-1022.

- Fritz, S.C., Baker, P.A., Lowenstein, T.K., Seltzer, G.O., Rigsby, C.A., Dwyer, G.S., and Luo, S., 2004, Hydrologic variation during the last 170,000 years in the southern hemisphere tropics of South America: *Quaternary Research* 61, 95–104, doi: 10.1016/j.yqres.2003.08.007.
- Garreaud, R. D., 2009. The Andes climate and weather. *Advances in Geosciences* 22, 3.
- Garreaud, R., Vuille, M., Clement, A. C., 2003. The climate of the Altiplano: Observed current conditions and mechanisms of past changes. *Paleogeography, Paleoclimatology, Paleoecology* 194, 5–22.
- Gosse, J.C., Phillips, F.M., 2001. Terrestrial in situ cosmogenic nuclides: theory and application. *Quaternary Science Reviews* 20(14), 1475-1560.
- Granger DE. 2006. A review of burial dating methods using ^{26}Al and ^{10}Be . *Geological Society of America Special Publication* 415, 1-16.
- Granger, D.E., Smith, A.L., 2000. Dating buried sediments using radioactive decay and muogenic production of ^{26}Al and ^{10}Be . *Nuclear Instruments and Methods in Physics Research*, B172, 822-826.
- Granger, D.E., Kirchner, J.W., Finkel, R.C., 1996. Spatially averaged long-term erosion rates measured from in situ-produced cosmogenic nuclides in alluvial sediment. *Journal of Geology* 104, 249-257.
- Granger, D.E., Muzikar, P.F., 2001. Dating sediment burial with in situ-produced cosmogenic nuclides: theory, techniques, and limitations. *Earth and Planetary Science Letters* 188, 269–281.
- Granger, D.E., Lifton, N.A., Willenbring, J.K., 2013. A cosmic trip: 25 years of cosmogenic nuclides in geology. *Geological Society of America Bulletin* 125(9-10), 1379-1402.
- Hancock, G.S., Anderson, R.S., 2002. Numerical modeling of fluvial strath-terrace formation in response to oscillating climate. *Geological Society of America Bulletin* 114(9), 1131-1142.
- Hidy, A.J., Gosse, J.C., Pederson, J.L., Mattern, J.P., Finkel, R.C., 2010. A geologically constrained Monte Carlo approach to modeling exposure ages from profiles of cosmogenic nuclides: An example from Lees Ferry, Arizona. *Geochemistry Geophysics, Geosystems* 11.
- Kohl, C.P., Nishiizumi, K., 1992. Chemical isolation of quartz for measurement of in-situ-produced cosmogenic nuclides. *Geochimica et Cosmochimica Acta* 56(9), 3583-3587.
- Korschinek, G., Bergmaier, A., Faestermann, T., Gerstmann, U.C., Knie, K., Rugel, G., 2010. A new value for the half-life of Be-10 by heavy-ion elastic recoil detection and liquid scintillation counting. *Nuclear Instruments and Methods in Physics Research Section B: Beam Interactions with Materials and Atoms* 268, 187-191.
- Lagos, P., Silva, Y., Nickl, E., Mosquera, K., 2008. El Niño? related precipitation variability in Perú. *Advances in Geosciences* 14, 231-237.

- Lal, D., 1991. Cosmic-ray labeling of erosion surfaces—In situ nuclide production-rates and erosion models. *Earth and Planetary Science Letters* 104, 424–439.
- Lisiecki, L.E., 2010. Links between eccentricity forcing and the 100,000-year glacial cycle. *Nature Geosci.* 3, 349–352.
- Litty C., Duller R., Schlunegger F., 2016. Paleohydraulic reconstruction of a 40 kyr-old terrace sequence implies that water discharge was larger than today. *Earth Surface Processes and Landforms* 41, 884–898. DOI: 10.1002/esp.3872.
- Litty, C., Lanari, P., Burn, M., Schlunegger, F., 2017a. Climate-controlled shifts in sediment provenance inferred from detrital zircon ages, western Peruvian Andes. *Geology* 45(1), 59–62.
- Litty, C., Schlunegger, F., Viveen, W., 2017b. Possible threshold controls on sediment grain properties of Peruvian coastal river basins. *Earth Surface Dynamics* 5, 1–13. <https://doi.org/10.5194/esurf-5-1-2017>
- McPhillips, D., Bierman, P.R., Rood, D. H., 2014. Millennial-scale record of landslides in the Andes consistent with earthquake trigger. *Nature Geoscience* 7(12), 925–930.
- NASA Land Processes Distributed Active Archive Center (LP DAAC). ASTER GDEM. USGS/Earth Resources Observation and Science (EROS) Center, Sioux Falls, South Dakota, 2001.
- Norris, T.L., Gancarz, A.J., Rokop, D.J., Thomas, K.W., 1983. Half-life of ^{26}Al . *Journal of Geophysical Research, Solid Earth* 88(S01).
- Norton, K.P., Schlunegger, F., Litty, C., 2016. On the potential for regolith control of fluvial terrace formation in semi-arid escarpments. *Earth Surf. Dynam* 4, 147–157, <https://doi.org/10.5194/esurf-4-147-2016>.
- Milankovitch, M. *Kanon der Erdbestrahlung und seine Anwendung auf das Eiszeitproblem* (R. Serbian Acad., 1941).
- Pederson, J.L., Anders, M.D., Rittenhour, T.M., Sharp, W.D., Gosse, J. C., Karlstrom, K.E., 2006. Using fill terraces to understand incision rates and evolution of the Colorado River in eastern Grand Canyon, Arizona. *Journal of Geophysical Research: Earth Surface* 111(F2).
- Pillans, B., Chappell, J., Naish, T.R., 1998. A review of the Milankovitch climatic beat: template for Plio–Pleistocene sea-level changes and sequence stratigraphy. *Sedimentary Geology* 122(1), 5–21.
- Placzek, C., Quade, J., Patchett, P.J., 2006. Geochronology and stratigraphy of late Pleistocene lake cycles on the southern Bolivian Altiplano: implications for causes of tropical climate change. *Geological Society of America Bulletin* 118, 515–532.
- Reber, R., Delunel, R., Schlunegger, F., Litty, C., Madella, A., Akçar, N., Christl, M., 2017. Environmental controls on ^{10}Be -based catchment-averaged denudation rates along the western margin of the Peruvian Andes. *Terra Nova*.

- Repka, J.L., Anderson, R.S., Finkel, R.C., 1997. Cosmogenic dating of fluvial terraces, Fremont River, Utah. *Earth and Planetary Science Letters* 152(1), 59-73.
- Steffen, D., Schlunegger, F., Preusser, F., 2009. Drainage basin response to climate change in the Pisco Valley, Peru. *Geology* 37, 491–494.
- Steffen, D., Schlunegger, F., Preusser, F., 2010. Late Pleistocene fans and terraces in the Majes Valley, southern Peru, and their relation to climatic variations. *International Journal of Earth Sciences* 99(8), 1975-1989.
- Stone, J.O., 2000. Air pressure and cosmogenic isotope production. *Journal of Geophysical Research: Solid Earth* 105(B10), 23753-23759.
- Strecker, M.R., Alonso, R.N., Bookhagen, B., Carrapa, B., Hilley, G.E., Sobel, E.R., Trauth, M.H., 2007. Tectonics and climate of the southern central Andes: *Annual Review of Earth and Planetary Sciences* 35, 747–787, doi: 10.1146/annurev.earth.35.031306.140158.
- Sylvestre, F., Servant, M., Servant-Vildary, S., Causse, C., Fournier, M., Ybert, J. P., 1999. Lake-level chronology on the Southern Bolivian Altiplano (18–23 S) during late-glacial time and the early Holocene. *Quaternary Research* 51(1), 54-66.
- Trauerstein M, Lowick SE, Preusser F, Schlunegger F. 2014. Small aliquot and single grain IRSL and post-IR IRSL dating of fluvial and alluvial sediments from the Pativilca Valley, Peru. *Quaternary Geochronology* 112, 163–174.
- Tucker GE, Slingerland R. 1997. Drainage basin response to climate change. *Water Resources Researc.* 33, 2031–2047.
- Veit, H., May, J.H., Madella, A., Delunel, R., Schlunegger, F., Szidat, S., Capriles, J. M., 2016. Palaeo- geoecological significance of Pleistocene trees in the Lluta Valley, Atacama Desert. *Journal of Quaternary Science* 31(3), 203-213.
- Von Blanckenburg F. 2005. The control mechanisms of erosion and weathering at basin scale from cosmogenic nuclides in river sediment. *Earth and Planetary Science Letters* 237(3), 462–479.
- Wolkowinsky, A.J., Granger, D.E., 2004. Early Pleistocene incision of the San Juan River, Utah, dated with ²⁶Al and ¹⁰Be. *Geology* 32(9), 749-752.

Tables and Figures captions

Table 1: Sample and cosmogenic nuclide data.

Table 2: Input parameters for the Monte Carlo simulator in Matlab® (Hidy et al., 2010).

Table 3: Results of the Monte Carlo simulations with Matlab® for (A) Barranca and (B) Pativilca. Total number of simulated profiles is 100,000. The bold numbers represent the modelled values and are therefore the ones that are used in this paper.

Table 4: Information relevant for interpreting ^{10}Be concentrations. Modern and paleo catchment-averaged denudation were calculated using the SRTM DEM with a 90 m resolution. A ^{10}Be half-life of 1.39 ± 0.01 Ma was used (Chmeleff et al., 2010; Korschinek et al., 2010) and a SLHL ^{10}Be production rate of $4.01 \text{ at g}^{-1} \text{ a}^{-1}$. A density of 2.65 g cm^{-3} was employed.

Fig. 1: (A) Maps of the study area showing the location of Pativilca and Barranca on the western side of the Peruvian Andes. (B) Field photographs showing the alluvial terraces in Barranca and Pativilca. Samples PAT-DP-1 to 6 (Pativilca), BAR-DP 1 to 6 (Barranca) were collected for depth-profile dating. The white lines represent the bracket level where quartz bearing clasts were sampled for isochron burial dating purposes. The concentrations obtained for the samples BAR-DP6 and PAT-DP6 were used for the calculation of the paleo-basin wide denudation rates

Fig. 2: Measured ^{26}Al concentrations plotted vs. ^{10}Be concentrations of the isochron-burial dating samples in Barranca (BAR-IS1, BAR-IS2 and BAR-IS3) and in Pativilca (PAT-IS1 and PAT-IS2). The sampling sites are shown on Fig. 1B. The errors represent 2σ uncertainties. The dash lines illustrate the surface production rate ratio of 6.75 (Balco et al., 2008).

Fig. 3: Measured ^{10}Be concentrations including the 1σ uncertainties of the Barranca depth-profile samples plotted against depth.

Fig. 4: Modal output of the Monte Carlo simulations showing frequency distributions and χ^2 values for exposure age, erosion rate and inheritance.

Fig. 5: Output of the Monte Carlo depth-profile age simulation. (A) Illustration of the best fit through the samples for the lowest χ^2 value. (B) Possible solution space with a χ^2 cut-off values of < 20 .

Fig. 6: Measured ^{10}Be concentrations including the 1σ uncertainties of the Pativilca depth-profile samples plotted against depth.

Fig. 7: Modal output of the Monte Carlo simulations showing frequency distributions and χ^2 values for exposure age, erosion rate and inheritance.

Fig. 8: Output of the Monte Carlo depth-profile age simulation. (A) Illustration of the best fit through the samples for the lowest χ^2 value. (B) Possible solution space with a χ^2 cut-off values of < 3 .

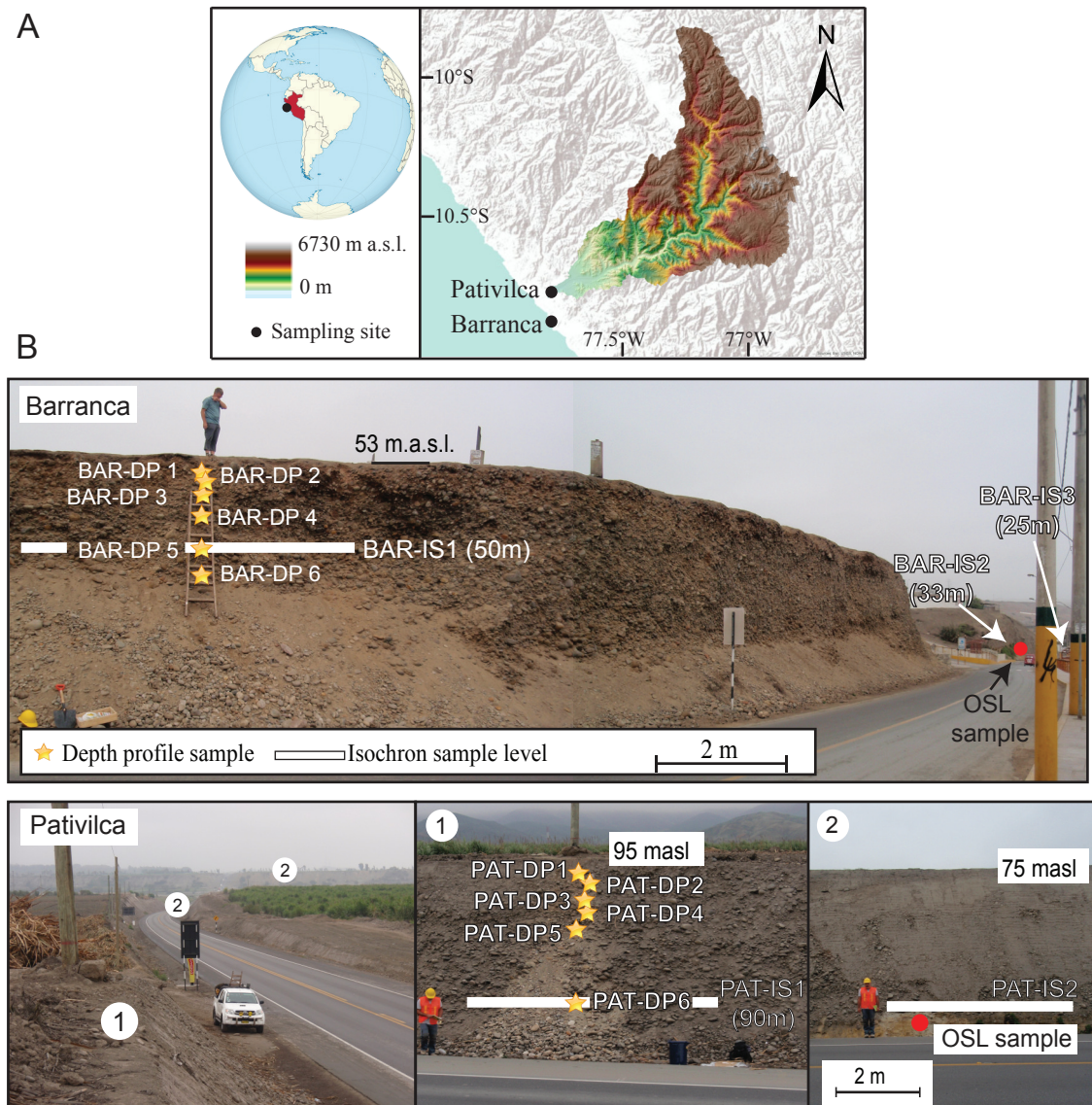
Fig. 9: Map of the alluvial terraces in Pativilca and Barranca showing the age of the different terraces.

Fig. 10: (A) Summary of the IRSL and depth-profile ages in Pativilca and Barranca. The black dots represent the IRSL samples from Trauerstein et al. (2014) and the white dot represents the depth profile (this study). (B) Summary of the paleo-catchment wide denudation rates. The transect A-B can be seen in Fig. 9.

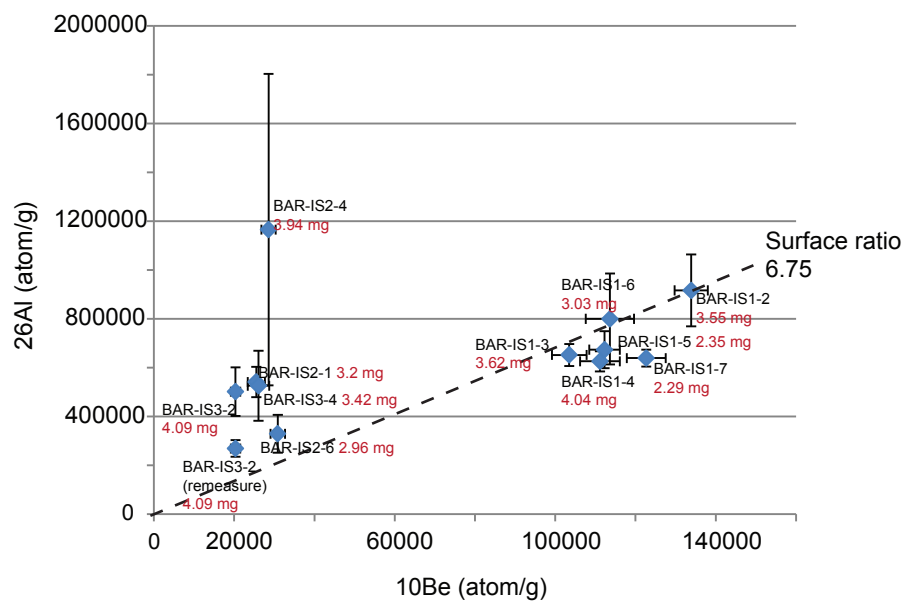
Fig. 11: Maps showing the inferred channel belt position during the sediment accumulation phases in the Pativilca Valley. (A) prior to ~ 1.2 Ma ago. (B) prior to ~ 200 ka ago. (C) ~ 100 ka ago. (D) ~ 30 ka ago.

Fig. 12: Erosion rates versus time.

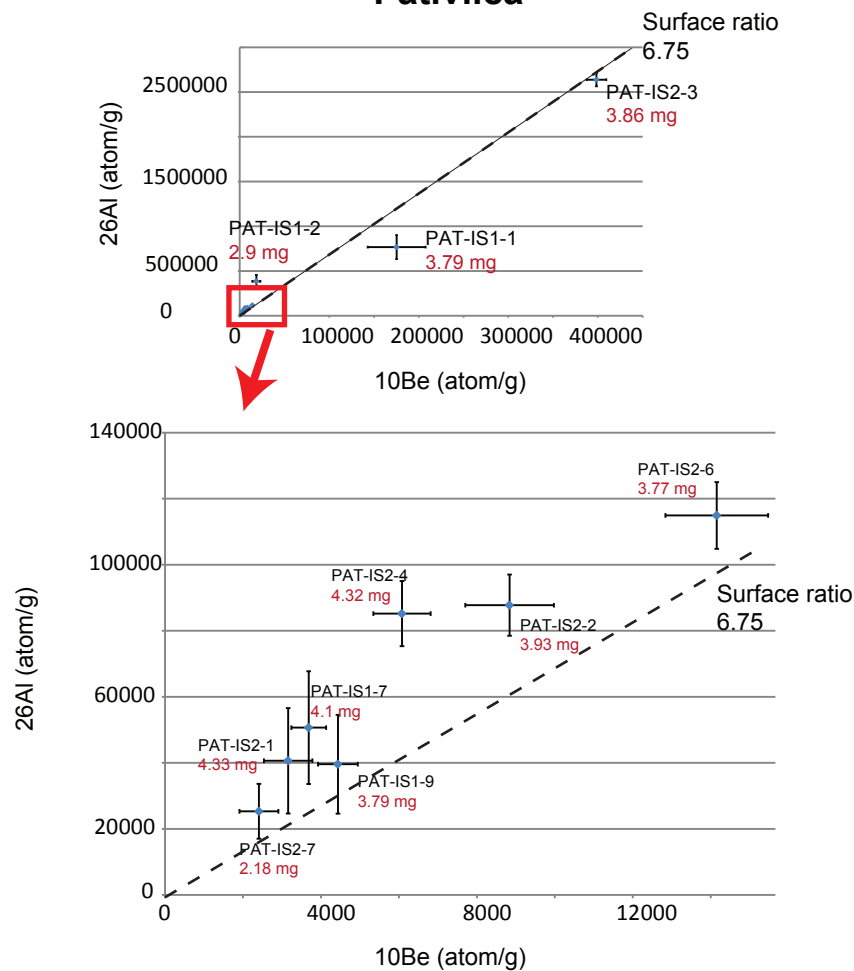
Figur
1



Barranca



Pativilca



Barranca Depth Profile (Peru)

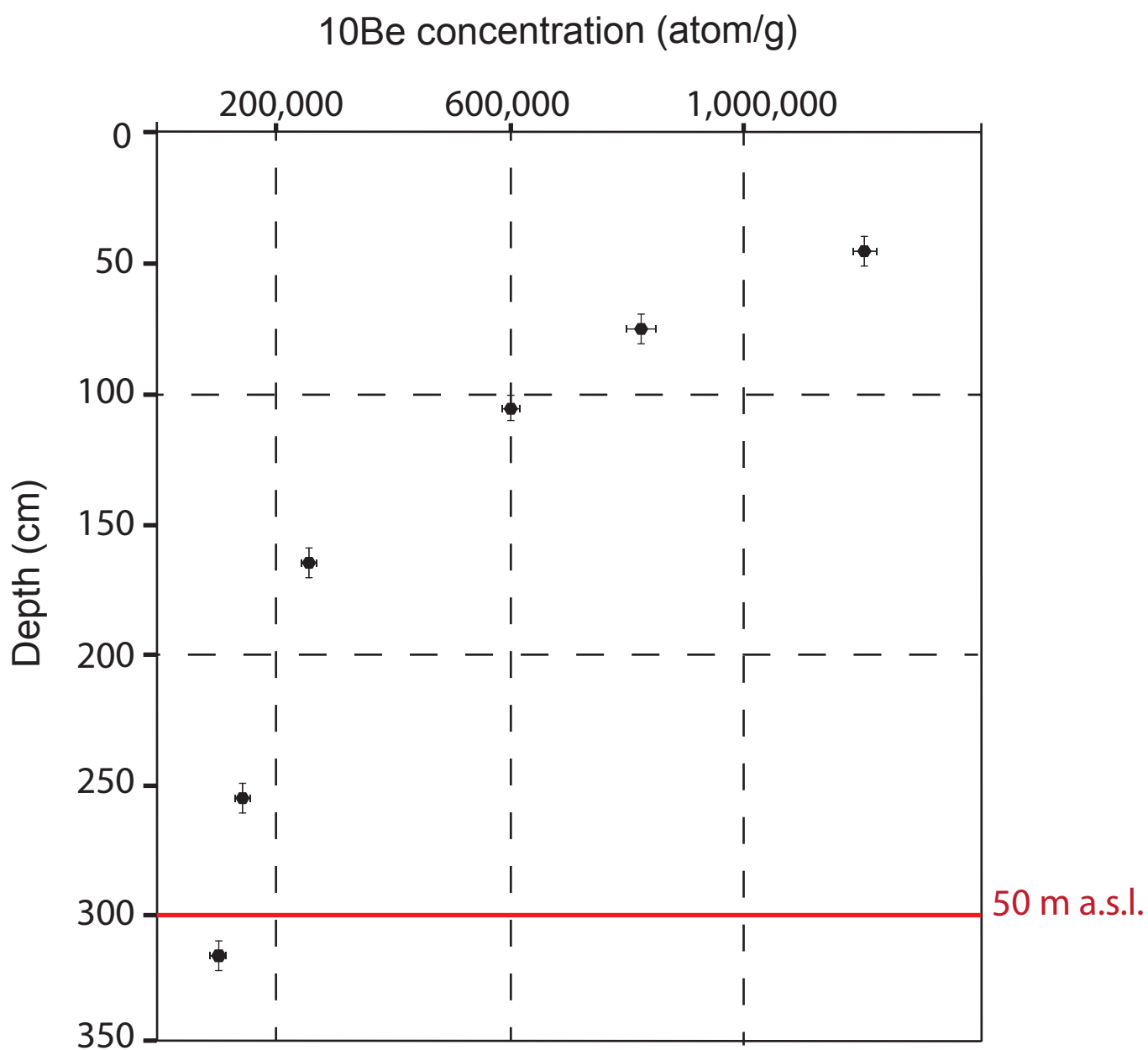
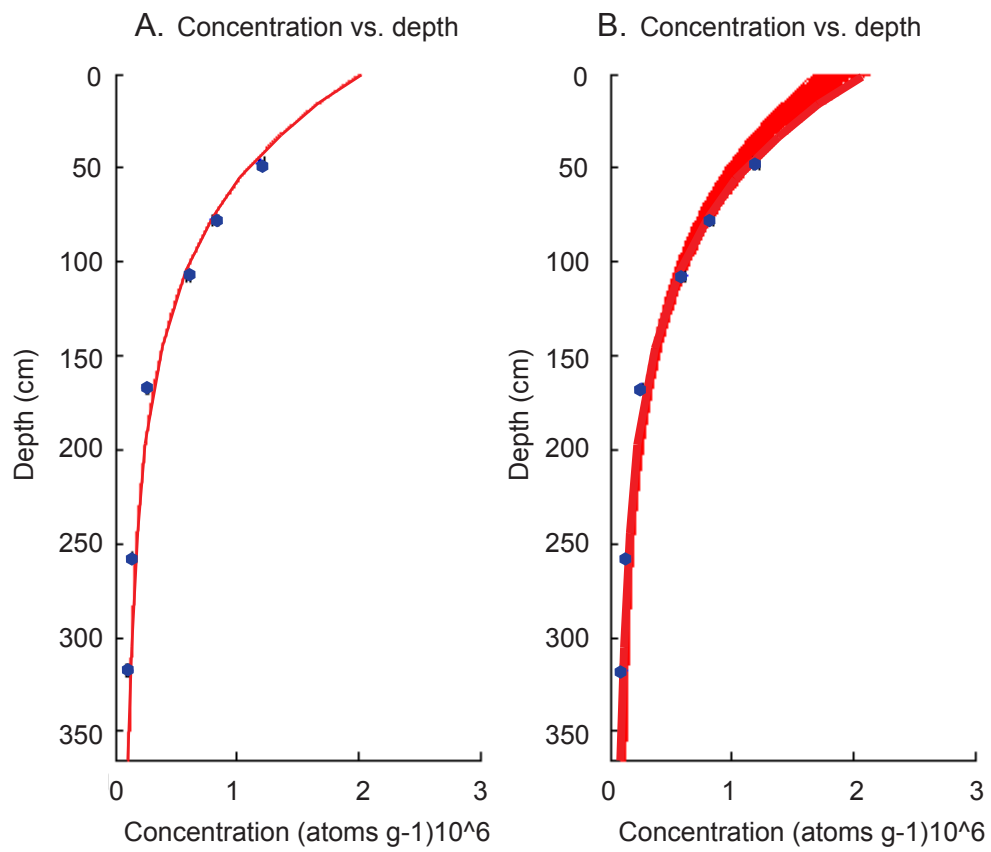
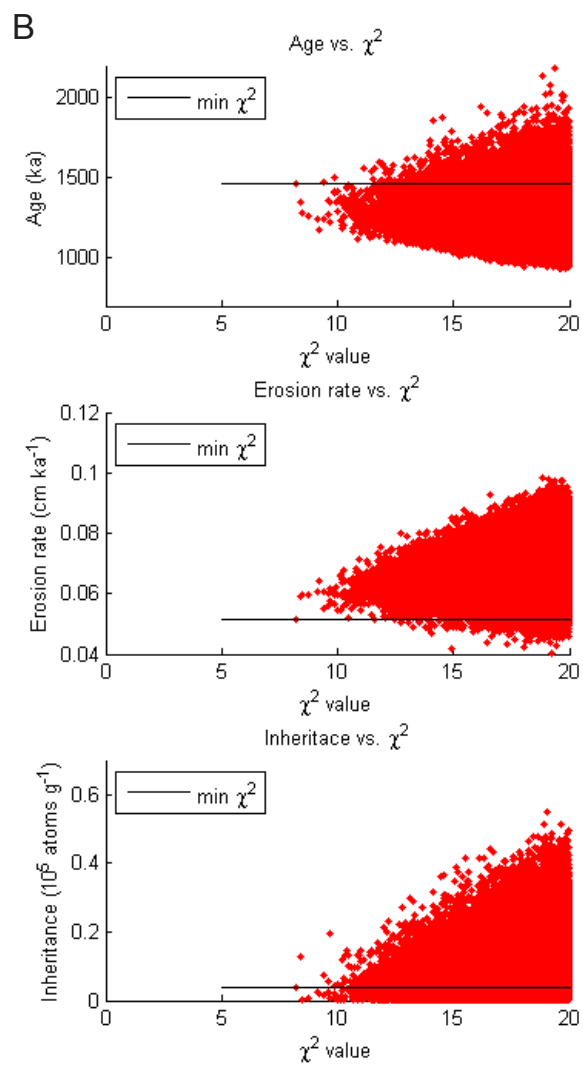
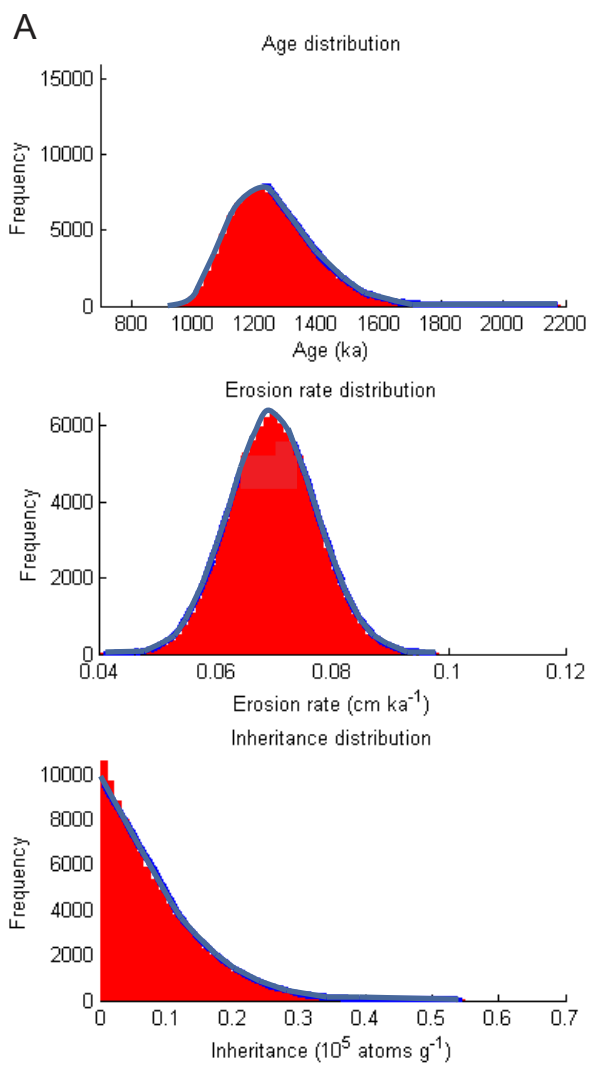
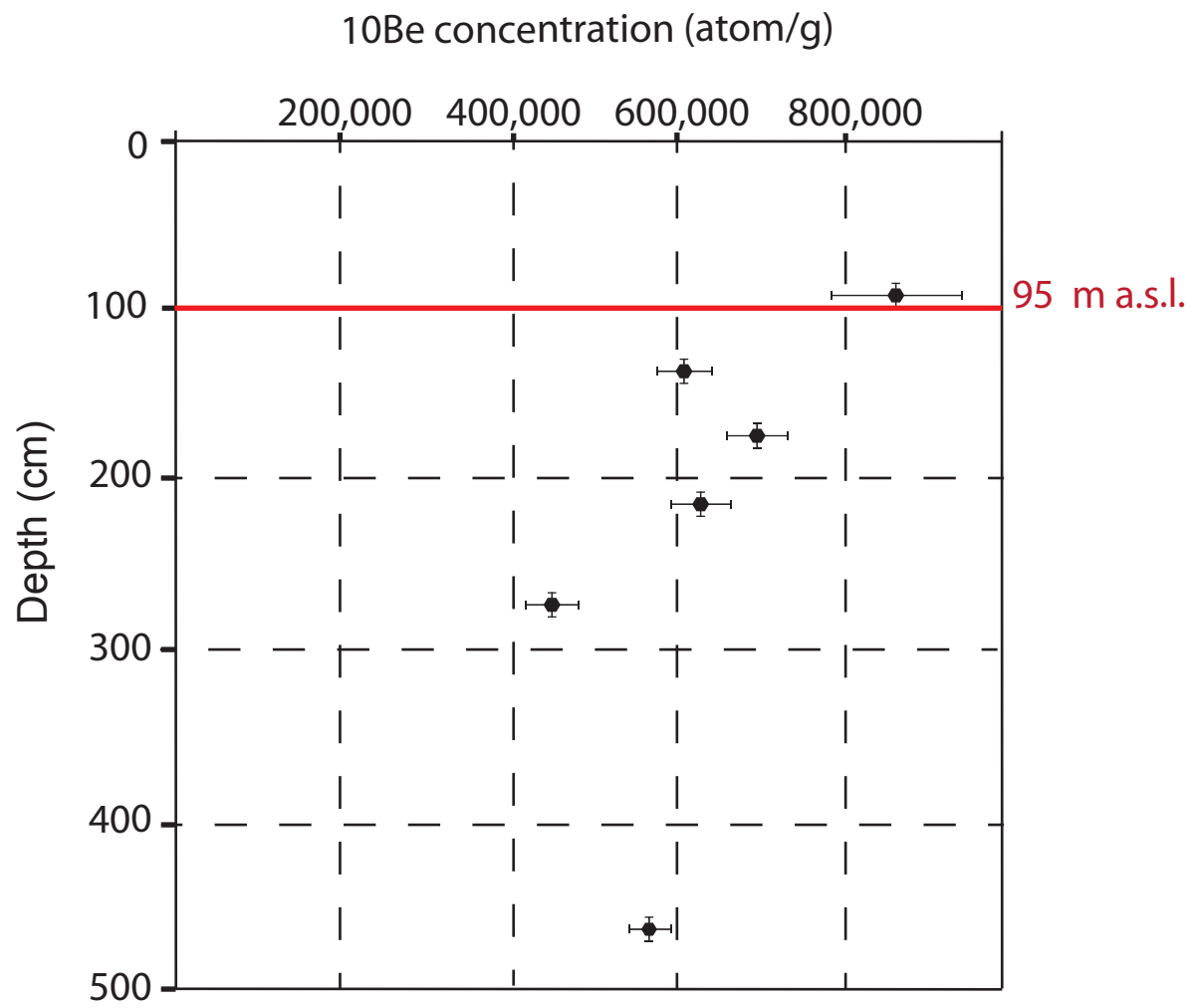
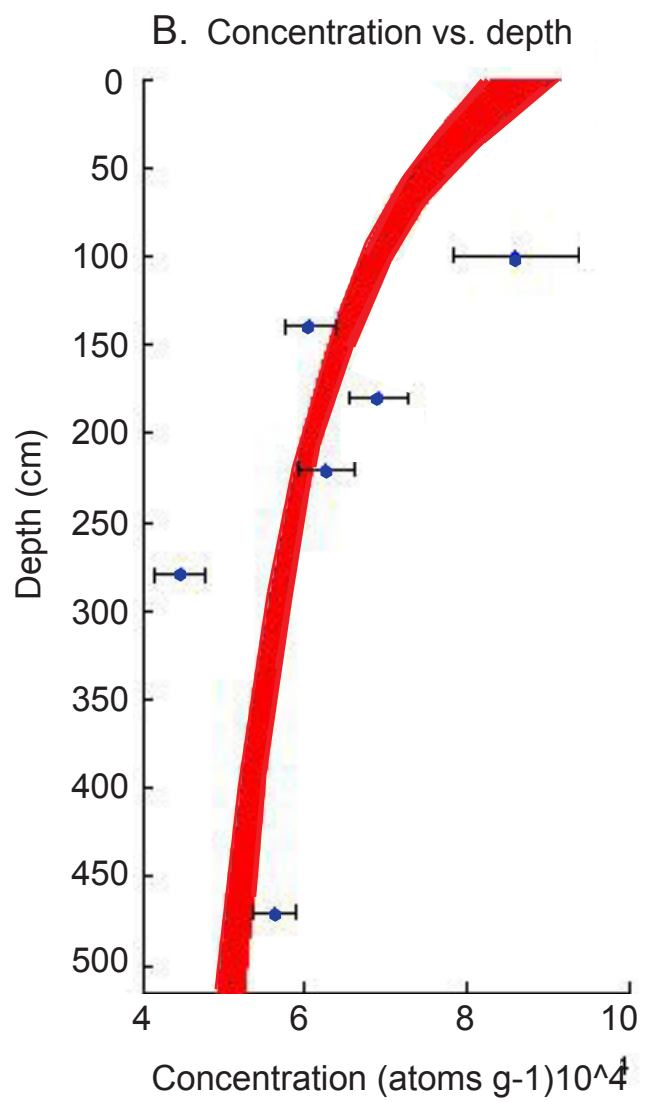
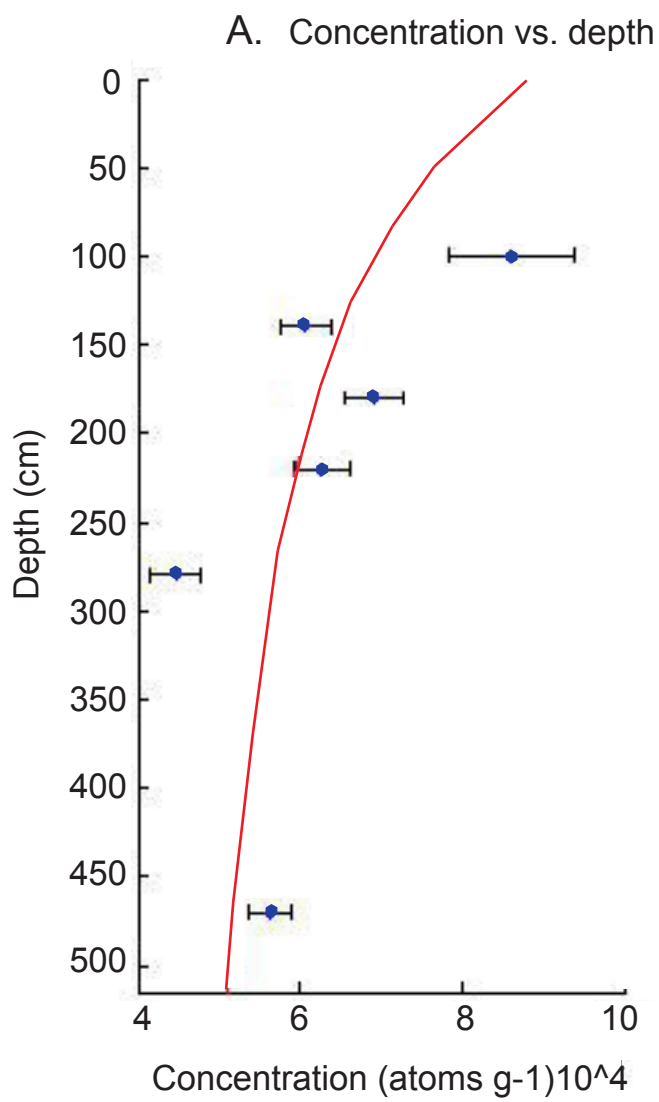


Figure 2

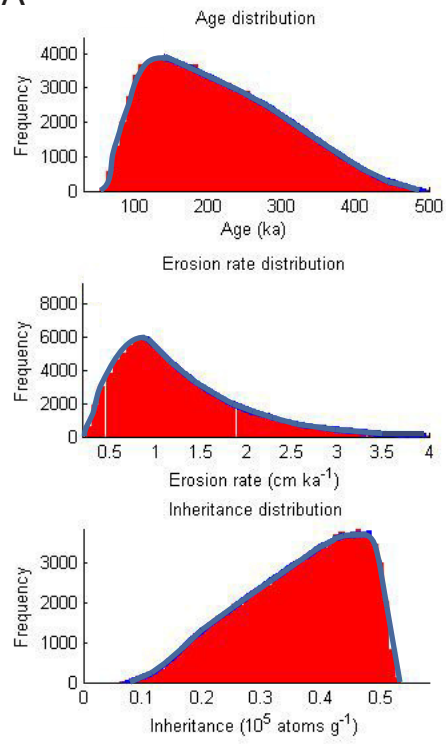








A



B

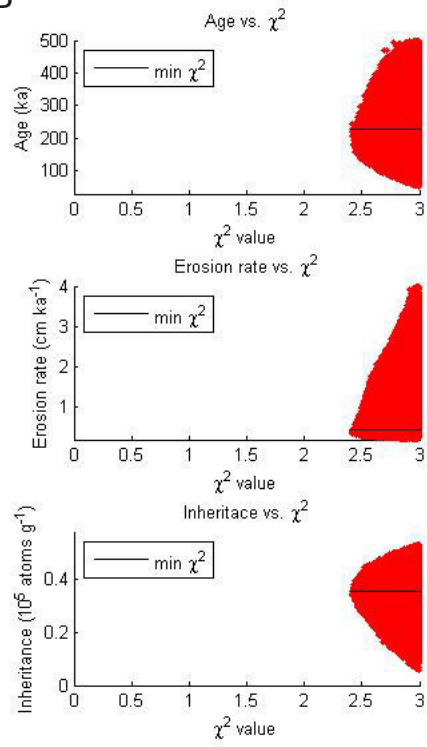
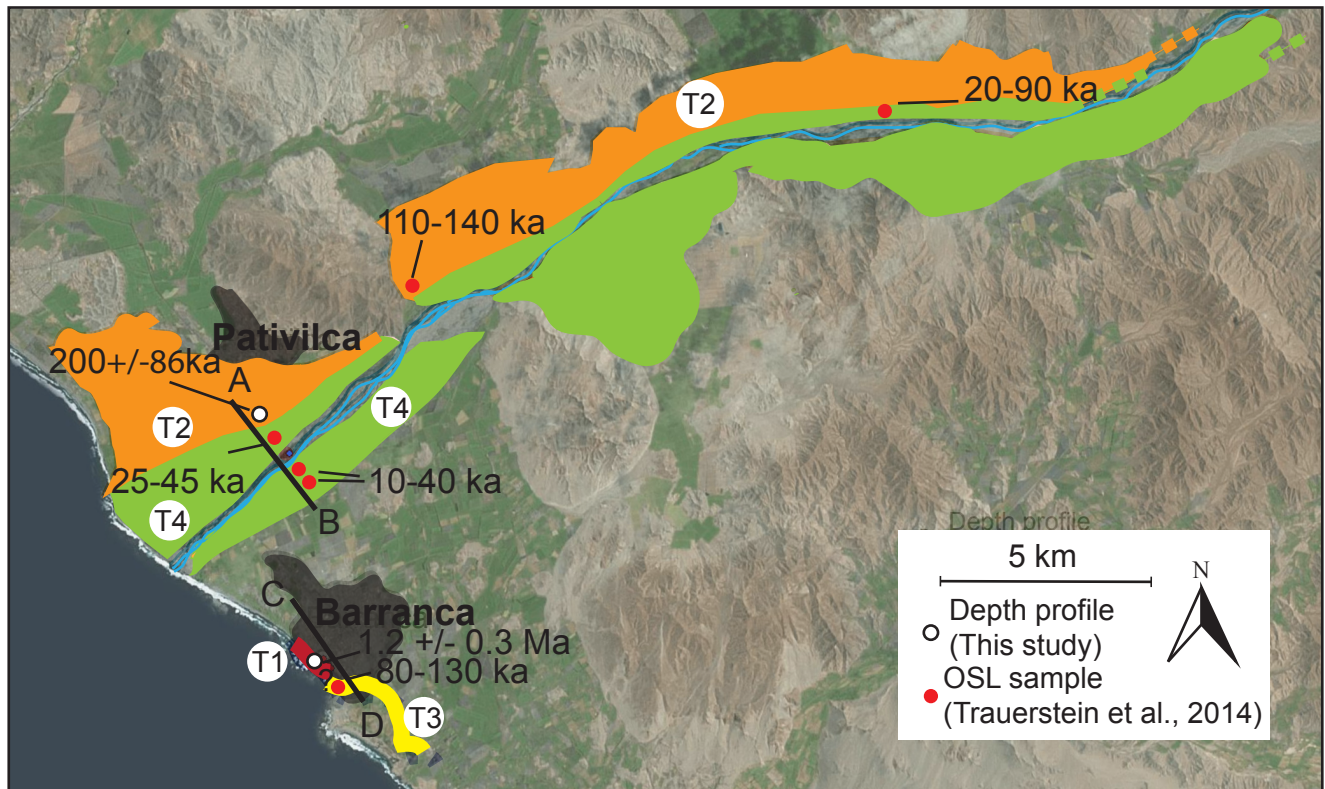
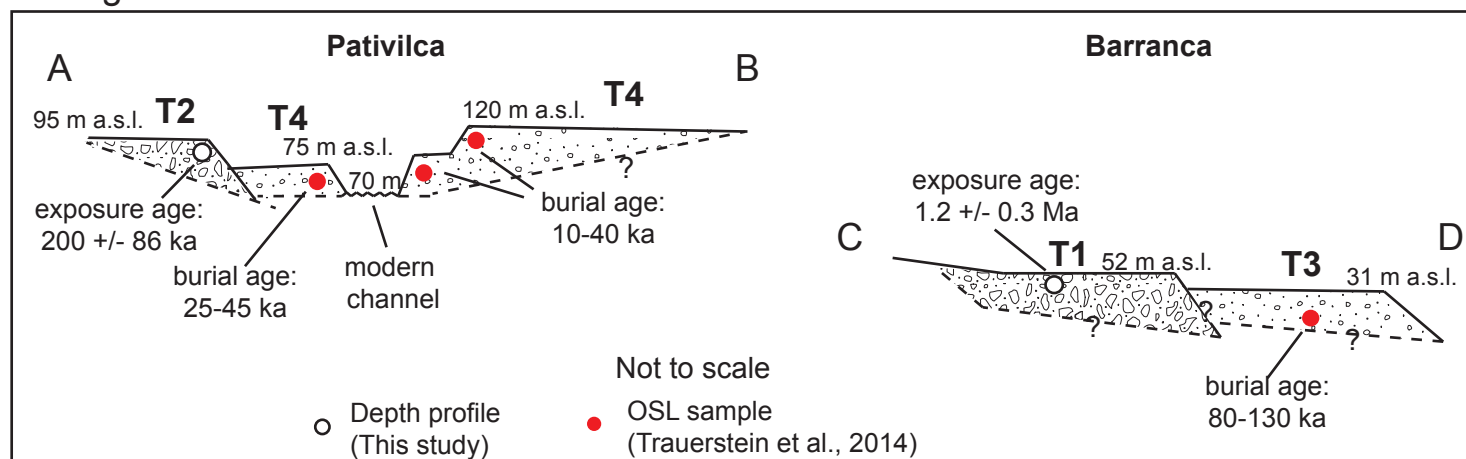


Figure 9



A. Ages



B. Erosion rates

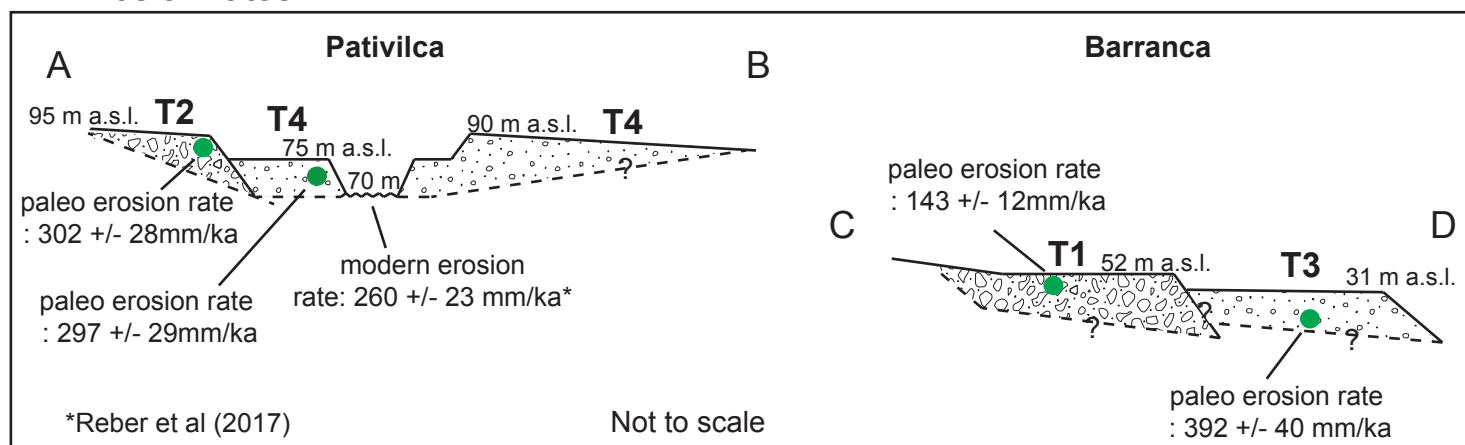


Figure
11

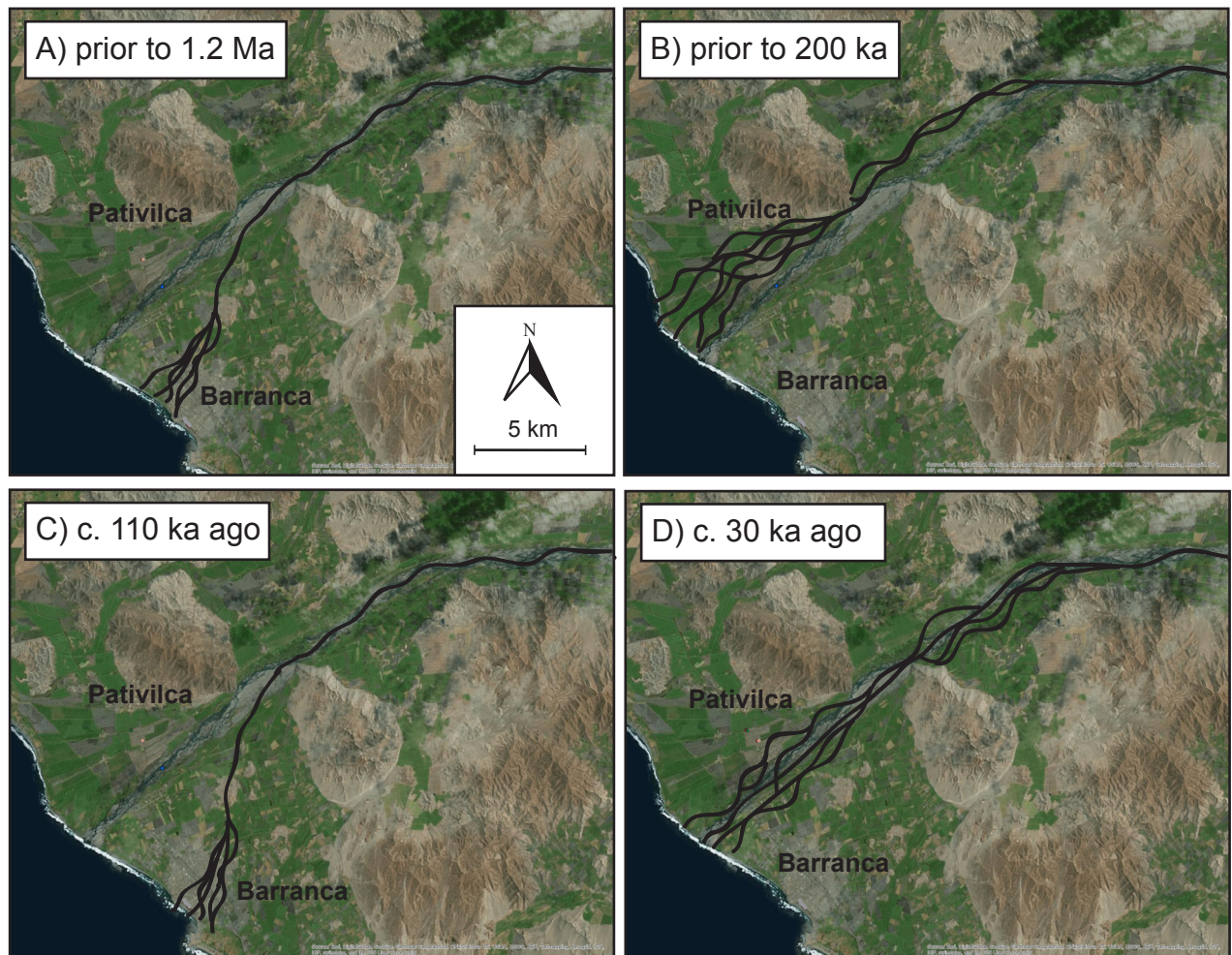


Figure
12

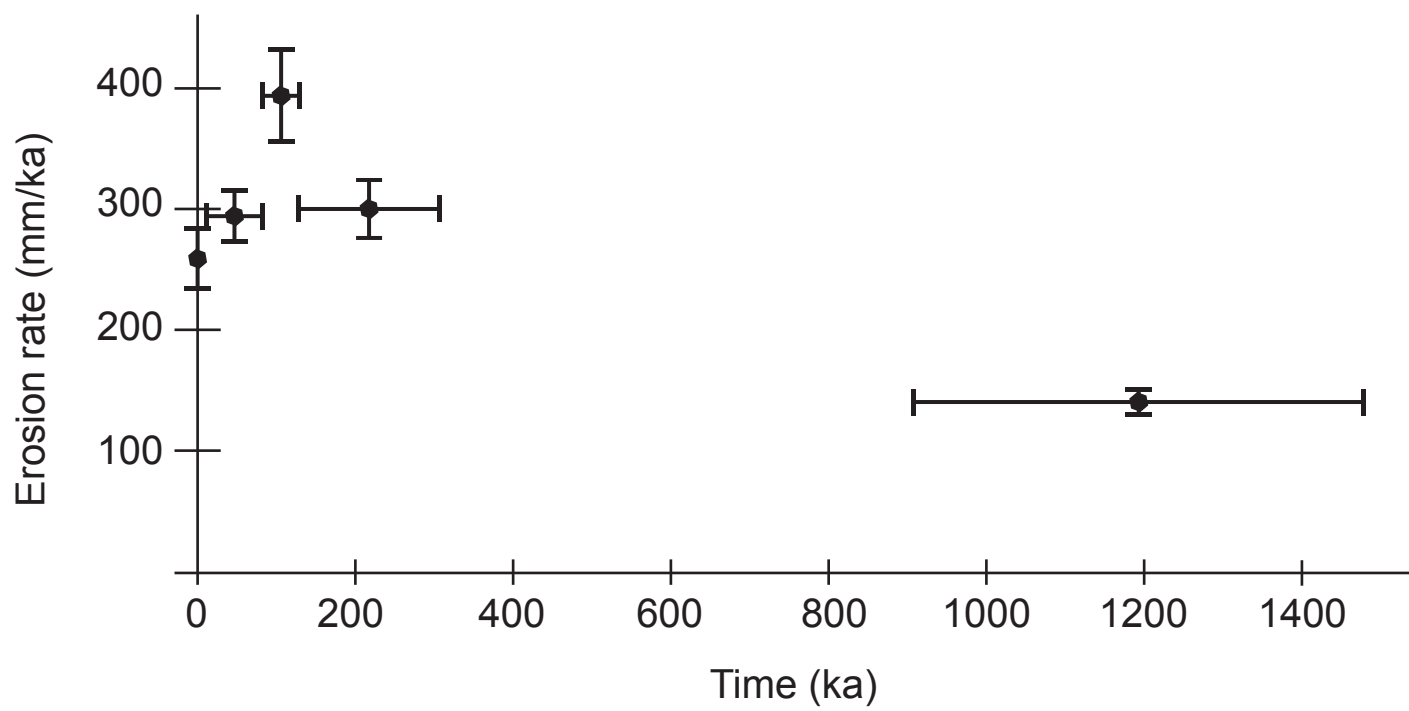


Table 1.
Sample information and cosmogenic nuclide data of the samples

Site	Technics	Latitude (°)	Longitude (°)	Altitude of the top of the terrace (m)	Sample name	Sample depth(cm)	Sample type	Quartz dissolved(g)	9Be spike(mg)	10Be/9Be	Relative uncertainty(%)	10Be concentration (10 ⁴ atoms/g)	Al(mg)	26Al/27Al	Relative uncertainty(%)	26Al concentration (10 ⁴ atoms/g)	26Al/10Be	Error on the ratio
Pativilca	Depth Profile dating	-10.704	-77.775	96	PAT-DP1	90-100	Sand	15.0271	0.1731	1,14E-13	8.72	8.59	n.d	n.d.	n.d.	n.d.	n.d.	n.d.
					PAT-DP2	130-140		49.8738	0.1702	2,68E-13	5.23	6.06						
					PAT-DP3	170-180		49.8325	0.1745	2,98E-13	5.18	6.91						
					PAT-DP4	210-220		50.0394	0.175	2,71E-13	5.38	6.26						
					PAT-DP5	270-280		49.9998	0.1725	1,96E-13	7.08	4.46						
					PAT-DP6	460-470		49.8804	0.1743	2,43E-13	4.64	5.62						
	Isochron burial dating	-10.704	-77.775	96	PAT-IS1-1	460-470	Quartz bearing clasts	38.207	0.1739	5,79E-13	18.4	17.5	3.79	3,46E-13	17,5	76.7	4.38	1.11
					PAT-IS1-2			38.7454	0.1737	6,45E-14	22.9	1.86	2.90	2,30E-13	18,6	38.5	20.7	6.24
					PAT-IS1-7			36.6074	0.1747	1,40E-14	9.96	0.368	4.10	2,03E-14	33,7	5.07	13.8	4.92
					PAT-IS1-9			37.689	0.1746	1,68E-14	9.81	0.443	3.79	1,76E-14	37,8	3.96	8.92	3.52
	Isochron burial dating	-10.708	-77.772	75	PAT-IS2-1	400-410	Quartz bearing clasts	39.5056	0.1737	1,32E-14	16.0	0.315	4.33	1,66E-14	39,3	4.06	12.8	5.65
					PAT-IS2-3			40.9181	0.1739	1,41E-12	2.73	3.98	3.86	1,25E-12	2,78	263	6.62	0.26
					PAT-IS2-7			36.3518	0.175	9,91E-15	15.6	0.241	2.18	1,89E-14	32,8	2.53	10.5	4.08
					PAT-IS2-2			32.5973	0.2004	2,39E-14	11.5	0.884	3.94	3,25E-14	10,6	8.77	9.93	1.65
					PAT-IS2-4			39.2653	0.1972	2,05E-14	10.6	0.608	4.32	3,47E-14	11,6	8.52	14.0	2.34
					PAT-IS2-6			39.8664	0.1998	4,47E-14	8.79	1.41	3.78	5,44E-14	8,79	11.5	8.12	1.04
Barranca	Depth Profile dating	-10.758	-77.765	53	BAR-DP1	40-50	Sand	36.2984	0.1661	3,94E-12	1.54	12.0	n.d	n.d.	n.d.	n.d.	n.d.	n.d.
					BAR-DP2	70-80		33.0576	0.1673	2,43E-12	3.04	82.1						
					BAR-DP3	100-110		25.7899	0.1731	1,34E-12	2.52	60.1						
					BAR-DP4	160-170		35.9971	0.1705	8,31E-13	3.02	26.2						
					BAR-DP5	250-260		50.2153	0.1747	6,08E-13	5.27	14.1						
					BAR-DP6	310-320		33.2556	0.1744	2,96E-13	4.41	10.3						
	Isochron burial dating	-10.758	-77.765	53	BAR-IS1-2	250-260	Quartz bearing clasts	37.67	0.1736	4,37E-13	3.07	13.4	3.55	4,35E-13	16.0	91.6	6.84	1.12
					BAR-IS1-5			25.9268	0.1718	2,36E-13	4.15	10.3	3.62	2,98E-13	6.92	65.2	6.30	0.71
					BAR-IS1-6			32.4907	0.1741	3,13E-13	4.44	11.1	4.05	2,85E-13	6.58	62.6	5.63	1.68
					BAR-IS1-3			37.025	0.2017	3,11E-13	3.38	11.2	2.36	3,32E-13	11.3	67.3	5.99	0.51
					BAR-IS1-4			41.1355	0.2023	3,48E-13	5.25	11.3	3.04	3,83E-13	23.3	79.9	7.03	0.45
					BAR-IS1-7			26.5406	0.2033	2,42E-13	3.91	12.3	2.29	3,31E-13	5.38	63.9	5.21	0.35
	Isochron burial dating	-10.759	-77.764		BAR-IS2-1	< 20 m	Quartz bearing clasts	40.3743	0.1737	9,12E-14	8.10	2.55	3.20	3,06E-13	11.5	54.1	21.2	3.02
					BAR-IS2-4			44.6497	0.1715	1,14E-13	5.99	2.85	3.94	5,91E-13	54.7	116.00	40.8	22.47
					BAR-IS2-6			37.5191	0.1742	1,02E-13	5.63	3.08	2.96	1,86E-13	23.5	32.9	10.6	2.58
	Isochron burial dating	-10.76	-77.763		BAR-IS3-2	< 25 m	Quartz bearing clasts	49.9169	0.1726	9,04E-14	5.68	2.03	4.09	2,74E-13	19.7	50.1	24.7	5.09
					BAR-IS3-4			45.1403	0.1737	1,04E-13	10.11	2.61	3.42	3,11E-13	27.3	52.6	20.2	5.89
					BAR-IS3-7			40.7863	0.1729	7,10E-14	8.56	1,94	3.62	2,79E-13	25.5	55.3	28.4	7.68

Table 2
Input parameters for the Monte Carlo simulator in Matlab (Hidy et al., 2010).

Barranca	
Parameter	Value
Latitude (degree)	-10,758
Longitutde (degree)	-77,765
Altitude (m)	53
Strike (degree)	0
Dip (degree)	0
Shielding correction factor	1
Cover correction factor	1
Uncertainty of 10Be Half-life (%)	1
Local spallogenic production rate (at g-1 a-1)	2,50
Error in local spallogenic production rate (at g-1 a-1)	± 0.5
Depth of muon fit (m)	6
Error in total production rate (%)	5
Density (g cm-3)	1.6-2.1
X2 value	20
Numbers of profiles	100,000
Age (a)	700,000-2,200,000
Erosion rate (cm ka-1)	0.04-0.12
Total erosion threshold (cm)	75-400
Inheritance (at g-1)	0-70,000
Attenuation length (g cm-2)	160 ± 5

Pativilca	
Parameter	Value
Latitude (degree)	-10,704
Longitutde (degree)	-77,776
Altitude (m)	96
Strike (degree)	0
Dip (degree)	0
Shielding correction factor	1
Cover correction factor	1
Uncertainty of 10Be Half-life (%)	1
Local spallogenic production rate (at g-1 a-1)	2,50
Error in local spallogenic production rate (at g-1 a-1)	± 0.5
Depth of muon fit (m)	6
Error in total production rate (%)	5
Density (g cm-3)	1.6-2.1
X2 value	3
Numbers of profiles	100,000
Age (a)	30,000-500,000
Erosion rate (cm ka-1)	0.2-4
Total erosion threshold (cm)	75-400
Inheritance (at g-1)	0-58,000
Attenuation length (g cm-2)	160 ± 5

A	Table Barranca		
	Results of the Monte Carlo simulations with Matlab		
	Age (ka)	Inheritance (atom/g)	Erosion rate (cm/ka)
Mean	1254.3	8300	0.07
Median	1239.4	6400	0.07
Mode	1197.1	300	0.07
Minimum X2	1261.5	1200	0.06
Maximum	1503.0	5,8000	0.09
Minimum	1043.2	0	0.05

B	Table Pativilca		
	Results of the Monte Carlo simulations with Matlab		
	Age (ka)	Inheritance (atom/g)	Erosion rata (cm/ka)
Mean	200.6	3,5500	0.52
Median	200.3	3,5500	0.51
Mode	204.1	3,5100	0.48
Minimum X2	217.6	3,7800	0.35
Maximum	314.3	4,3800	0.89
Minimum	125	2,7100	0.25

Sample name	Paleo/modern erosion rates	Age of the deposits	Latitude (DD.DD) WGS84	Longitude (DD.DD) WGS84	Altitude of the top of the terrace (m.a.s.l)	Sample depth (cm)	Quartz dissolved (g)	9Be spike (mg)	Measured 10Be/9Be ratio (10 ⁻¹²)	AMS error (%)	10Be concentration (at/g)	Concentration at the time of deposition (at/g)	Denudation rates (mm/ka)
PAT-ME	Modern erosion rates	Modern Pativilca river	10.717°S	77.767°W	71	Surface	50.11	0.1991	0.24	4.0	6,4052 +/- 2695	6,4052 +/- 2695	260 +/- 23
PAT-DP6	Paleo erosion rates	Terrace T1 (Pativilca) : 200 ka	10.704°S	77.775°W	95	465 cm	49.88	0.1743	0.24	4.6	5,6219 +/- 2634	5,5203 +/- 2539	302 +/- 28
PAT-PE	Paleo erosion rates	Terrace T3 (Pativilca) : 40 ka	10.708°S	77.772°W	75	400 cm	49.97	0.1953	0.22	5.5	5,6468 +/- 3144	5,6004 +/- 3080	297 +/- 29
BAR-DP6	Paleo erosion rates	Terrace (Barranca) : 1.2 Ma	10.758°S	77.765°W	52	315 cm	33.25	0.1744	0.30	4.4	10,2942 +/- 4574	11,6020 +/- 2464	143 +/- 12
BAR-PE2	Paleo erosion rates	Terrace (Barranca) : 100 ka	10.759°S	77-764°W	33	400 cm	41.24	0.1984	0.14	6.3	4,4416 +/- 2823	4,2570 +/- 2682	392 +/- 40